RESEARCH ARTICLE   **OPEN ACCESS**

EXOGENOUS SURFACTANT PREVENTS THE MITOCHONDRIAL DEPOLARIZATION AND CHANGES IN CALCIUM HOMEOSTASIS DUE TO OXIDATIVE STRESS THAT LEADS TO APOPTOSIS IN EXPERIMENTAL LUNG INJURY

Neha Mittal and Sankar Nath Sanyal*

Department of Biophysics, Panjab University, Chandigarh-160014, INDIA

ABSTRACT

Background: *Apoptosis has been considered as an underlying mechanism in acute lung injury/acute respiratory distress syndrome. Recently, several alternative pathways such as the mitochondrial membrane depolarization for cell death have been discovered.* **Objectives:** *The present study investigated the role of surfactant therapy during LPS mediated changes in intracellular calcium concentration ([Ca]i) and mitochondrial depolarization as a possible intermediate in apoptosis.* **Methods:** *Adult male Sprague Dawley rats were divided into four groups: buffer controls; rats challenged with LPS (055:B5 E.coli); challenged with LPS and treated with porcine surfactant (P-SF); and challenged with LPS and treated with synthetic surfactant (S-SF). Experiments with surfactant were performed 72h after treatment with LPS.* **Results:** *To ascertain the mechanism of BALF cell apoptosis, we observed that LPS treatment induced oxidative burst, dissipated mitochondrial membrane potential, induced alteration of Ca^{2+} homeostasis and enhanced apoptosis. These effects were largely prevented by exogenous surfactant preparation.* **Conclusion:** *The anti-inflammatory activity may occur through an interaction with downstream signaling elements and Ca^{2+} influx. The findings show the importance of Ca^{2+} ions in regulating the response of BALF cells to oxidative stress that triggers downstream signaling cascades leading to the apoptosis. Therefore, treatments aimed at diminishing the damage to lung derived cells might become a key element in accelerating recovery and lead to the development of novel therapies for acute lung injury.*

***Corresponding author:** Email: sanyalpu@gmail.com, sanyal@pu.ac.in; Tel: +91-0172-2534122

[I] INTRODUCTION

Acute lung injury (ALI) and its more severe form, acute respiratory distress syndrome (ARDS), represent a clinical syndrome that results from complex responses of the lung to a multitude of direct and indirect insults. The different types of cell death that occur and the underlying mechanisms utilized depend on both experimental and clinical conditions [1]. Lipopolysaccharide (LPS) induced acute lung injury generates reactive oxidative species, which induce complex cell death patterns composed of apoptosis, and necrosis.

Apoptosis is a process of cell death in which the cells undergo nuclear and cytoplasmic shrinkage; the chromatin is condensed and partitioned into multiple fragments, and finally the cells are broken into multiple membrane-bound bodies. In a number of experimental systems, disruption of mitochondrial transmembrane potential ($\Delta\Psi m$) constitutes a constant early event of the apoptotic process that precedes nuclear disintegration [2]. $\Delta\Psi m$ loss can be brought about by reactive oxygen species (ROS) added directly in vitro or generated by agents that affect cellular metabolism [3]. A number of molecular targets of reactive oxygen species (ROS) have been

identified, including membrane phospholipids, transporters, enzymes, transcription factors, DNA, etc. [4]. Respiratory chain dysfunction could also lead to increased ROS production and formation of a vicious cycle, thereby killing cells either necrotically, apoptotically, or by some combination thereof [5]. Key features within the apoptosis cascades are dissipation of mitochondrial membrane potential, increased mitochondrial oxidant production, and apoptogenic protein release [6].

On the other hand, elevation of the cytosolic free Ca^{2+} ($[Ca^{2+}]_c$) level is suggested to participate in the activation of nucleases that are involved in chromatin organization, induce gene expression and also cleavage of nuclear DNA activated by nucleases during programmed cell death or apoptosis [7]. The role of elevated $[Ca^{2+}]_c$ in bringing about early apoptotic changes including $\Delta\Psi m$ loss in a cell is evident from studies showing the ability of intracellular Ca^{2+} chelators to block apoptosis [8] and the proapoptotic changes that can be induced by Ca^{2+}-mobilizing agents responsible for the release of Ca^{2+} from the endoplasmic reticulum [9]. In some cell systems, it is

IIOAB-India

Mittal et al. IIOABJ; Vol. 3; Issue 1; 2012: 3–10

3

not only the $[Ca^{2+}]_c$ increase but mitochondrial Ca^{2+} ($[Ca^{2+}]m$) overload [10] as well that precipitates a decrease in $\Delta\Psi m$.

Clinical investigations have demonstrated that replacement therapy with exogenous surfactant is effective for patients with ARDS [11]. Administration of surfactant *in vivo* inhibited the mitochondrial pathway of caspase-mediated apoptosis triggered by LPS [12] or by a variety of stimuli, such as inflammatory cytokines, growth factors, reactive oxygen species, and others, which are also involved in this model [13, 14]. Our earlier work has shown that surfactant therapy was proved to be effective during inflammatory responses in endotoxin induced ARDS [14, 15]. It seems reasonable therefore, that exogenous surfactant may improve surfactant function either by supplementing the lack of endogenous surfactant or by neutralizing the surfactant inhibitors, but the mechanism(s) on the effectiveness of exogenous surfactant on ARDS are not fully elucidated.

Together, the existing literature suggests that the alterations of Ca^{2+} levels in cell cytoplasm and mitochondria brought about by ROS or other agents can serve as critical signaling components leading to the activation of the apoptotic pathway. Therefore, we have focused our interest on the oxidative stress, mitochondrial membrane potential, cytosolic Ca^{2+} levels, and cell death seen in BALF cells in a rat model of ARDS induced by intratracheal instillation of LPS and subsequently treated with exogenous surfactant.

[II] MATERIALS AND METHODS

2.1. Animal modal

Male rats of Sprague Dawley (SD) strain, weighing 150-200g were taken from the Central Animal House of Panjab University and kept in polypropylene cages and supplied with pellet diet and drinking water ad libitum. Control animals were administered with 300µl of the buffer (50mM Tris-HCl, pH-7.4, 150mM NaCl, 1mM NaN3, 0.2mM PMSF). For LPS animals, endotoxin (150µg of 055:B5 E.coli LPS, Sigma Aldrich, USA) was suspended in 300µl of surfactant buffer. All rats were anesthetized with ketamine (130mg/kg. i.p.), such that they remained unconscious throughout the entire instillation procedure and had no cough reflex upon intubation. A small incision was made on the ventral region of the neck and the trachea carefully exposed. Animals were then placed on a slight incline, intubated with a 26-gauge needle and either buffer or LPS instilled followed by 2-3 boluses of 1ml air to facilitate the distribution of the instilled fluid. Shortly thereafter, when normal spontaneous breathing was apparent, the neck incision was closed with silk sutures. To avoid any infection betadine and neosporin powder were applied to the wound area. Two hours prior to killing, surfactant isolated from porcine (0.5mg protein + 0.86mg lipid/300µl) or synthetic surfactant (6.95mg lipid/300µl) were intratracheally instilled in P-SF and S-SF groups respectively, after LPS administration following the identical instillation procedure. The animals were sacrificed at 72 hours after buffer or LPS instillation [14]. All of the animal procedures as reported here had been carried out following the guidelines approved by the Panjab University Ethical Committee on the use of the experimental animals for biomedical research.

2.2. Surfactant preparation

Surfactant was isolated from porcine lung homogenate (P-SF) by sucrose density gradient method [16] while protein free synthetic surfactant (S-SF) was prepared with 13.9mg/ml dipalmitoylphosphohatidyl choline (DPPC), 1.5mg/ml hexadecanol and 1.0mg/ml Tyloxapol [16].

2.3. Bronchoalveolar lavage fluid (BALF) isolation

At the end of each experiment, a bronchoalveolar lavage was performed using 5ml phosphate buffered saline (PBS, pH-7.4). The average fluid recovery was greater than 90%. The recovered volume was centrifuged at 1000 rpm for 10 min at 40C and the supernatants were stored at -20^0C until analysis. Differential counts were performed on 200 cells stained with Wright Giemsa [13].

2.4. Measurement of intracellular ROS

To monitor the level of ROS, the cell-permeating probe DCFH-DA was used [14] whose fluorescence was found to be proportional to the amount of ROS formed intra-cellularly. Cells were incubated in dark conditions with the DCFH-DA dye (2.5µM) and with Hoechst 33342 for 15 min at 37^0C for counter staining and the cell suspension were placed on glass slide for observation under fluorescence microscope at 400 X (Axioscope, A1, Carl Zeiss, Germany).

2.5. Measurement of mitochondrial membrane potential changes

$\Delta\Psi m$ was estimated using JC-1 as a probe according to the method of Dey and Moraes [17] with slight modifications. Briefly, cells (1×10^6) were incubated for 7 min with 10µM of JC-1 at 37°C, washed, resuspended in PBS and measured for fluorescence in a fluorescence spectrometer. The ratio of the reading at 590 nm to the reading at 530 nm (590:530 ratio) was measured as the relative $\Delta\Psi m$ value. For microscopy, JC-1-stained cells were placed on slides and immediately imaged with the fluorescence microscope using the X40 objective. Aggregates of JC-1 are retained in intact mitochondria and fluoresce red, whereas mitochondria that have undergone a permeability transition release the JC-1 monomers into the cytoplasm, where they fluoresce green. Similarly, cells were incubated at 37^0C for 15 min with rhodamine 123 at a concentration of 10µM, washed and resuspended in PBS (pH-7.4), and measured for fluorescence at 488nm excitation and 536 nm emission. For microscopy, cells were incubated with dye, washed similarly as mentioned above and resuspended in 50µl PBS and placed on slides for viewing under fluorescence microscope at 400X.

2.6. Measurement of intracellular calcium mobilization

To evaluate whether LPS and surfactant cause mobilization of intracellular calcium, we used the fluorescent indicator chlortetracycline (CTC). CTC exists as neutral and ionic forms, and the anionic form complexes with cations (Ca^{2+}). An increase in fluorescence emission by up to two orders of magnitude occurs when CTC binds to the membrane-associated Ca^{2+}, as compared to the fluorescence of CTC alone. The cell suspension was incubated with 10µM CTC for 5 min at 37^0C using excitation 390 nm, emission 520 nm. Changes in luminal Ca^{2+} are expressed as changes in the intensity of CTC fluorescence [18]. For microscopy, cells were incubated with CTC and propidium iodide (as counter stain) and the 10µl suspension was placed on glass slide, covered with cover slip and observed under the fluorescence microscope.

IIOAB-India

Mittal et al. IIOABJ; Vol. 3; Issue 1; 2012:3–10

4

2.7. Measurement of cytosolic free Ca^{2+} concentrations

Changes in intracellular Ca^{2+} concentration $[Ca^{2+}]i$ were monitored with the fluorescent probe FURA-2/AM as described by Grynkiewicz et al. [19] with slight modifications. Cells (1×10^6 /ml) were loaded with 1μM fura-2/AM (1μg/μl in DMSO) for 30 min at 37^0C, to allow loading of the dye. The cells were collected by centrifugation at 500 g for 10 min at 4^0C, and resuspended in the PBS (pH 7.4). Fluorescence measured at excitation wavelengths of 340nm and 380nm, and an emission wavelength of 510nm. Ratios (R) of fluorescence intensity (F) of F340/F380, were measured for which the fractional changes in $[Ca^{2+}]i$ determined [19]. The fluorescence after sequential addition of SDS (20%) and 0.5M EGTA (pH 8) to the cell suspension provided the maximum fluorescence ratio (Rmax) and minimum fluorescence ratio (Rmin), respectively. To convert fluorescence values into absolute $[Ca^{2+}]i$, calibration was performed at the end of each experiment. $[Ca^{2+}]i$ was calculated using the following equation: $[Ca^{2+}]i = Kd[(R-Rmin)/(Rmax-R)]$, [19] where Kd is the dissociation constant of the FURA-2 complex (225nM), and R is the ratio of the fluorescence intensities measured at 340 and 380nm. Rmax is the same ratio when saturated with Ca^{2+} (after the addition of SDS), while Rmin is the same ratio in the absence of Ca^{2+} (after the sequential addition of EGTA)

2.8. Quantification of apoptotic cells

An annexin V–fluorescein isothiocyanate (FITC) kit (TACS® Annexin V Kits, Trevigen Inc. Gaithersburg, MD) was used to quantify apoptotic cells in accordance with manufacturer's procedure and examined for Annexin V-fluorescein isothiocyanate and propidium iodide (PI) fluorescence under fluorescence microscope.

2.9. Statistical analysis

Statistical analysis was performed using SPSS version 10.0 software. One way analysis of variance (ANOVA) was done to compare the means between the different treatments using Post-Hoc comparison by Least Significant Difference (LSD) method. A value of $p < 0.05$ was considered significant in the present study. All data were expressed as Mean ± SD of five animals for each group.

[III] RESULTS

3.1. LPS generated oxidative burst

H_2DCFDA is a nonpolar compound that readily diffuses into the cells, where it is hydrolyzed to the nonfluorescent derivative dichlorodihydrofluorescein and is thereby trapped within the cells. In the presence of a proper oxidant, dichlorodihydrofluorescein is oxidized to the highly fluorescent 2,7-dichlorofluorescein. We analyzed the DCFH-DA stained cells with a fluorescence microscope for all the treatment groups. **Figure– 1(a)** shows the morphological changes that occur in the BALF cells after exposure to the oxidative stress. 13.25% of the control cells fluoresce blue due to the uptake of Hoechst 33342 dye, indicating less oxidative stress. After exposure to LPS, an increased number of cells show a heterogeneous staining pattern and 73.2% (p<0.001) of the cells show DCFH-DA dye uptake and fluoresce green (indicated with arrows), whereas 34.25% (p<0.001) of cells were seen positive in LPS+P-SF group and 46.5% (p<0.001) of cells in LPS+S-SF

group which means the oxidative stress is less prevalent in surfactant treated groups as compared to the LPS treated group **[Figure– 1b]**.

3.2. Changes in mitochondrial membrane potential

JC-1 is a cationic mitochondrial dye that is lipophilic and becomes concentrated in the mitochondria in proportion to their ΔΨm; more dye accumulates in mitochondria with greater ΔΨm and ATP-generating capacity. Therefore, the fluorescence of JC-1 can be considered as an indicator of relative mitochondrial energy state. The dye exists as a monomer at low concentrations (emission 530 nm, green fluorescence) but at higher concentrations forms J-aggregates (emission 590 nm, red fluorescence). Exposure to LPS induced a significant reduction (1.13 ± 0.04, p<0.001) of mitochondrial membrane potential in BALF cells when compared with control rats (10.72 ± 0.86, **Figure– 2b**). Accumulation of JC-1 dye in the aggregated form (red fluorescence) was observed in the mitochondria of control cells **[Figure– 2a]**. In contrast, after exposure to LPS monomeric dye dispersed in the cytoplasm and displayed green fluorescence indicating the collapse of mitochondrial membrane integrity. Surfactant treated groups had a distinct pattern of staining with areas of both red and green that overlapped as yellow indicating a very close placement of regions with high and low ΔΨm. Cytoplasmic appearance of monomeric JC-1(green fluorescence) seen in the LPS+ surfactant group was less prevalent (6.73 ± 0.69 in P-SF group and 3.85 ± 0.35 in S-SF, p<0.001) than that detected in LPS treated animals.

Rhodamine fluorescence was clearly seen in control and surfactant treated cells **[Figure–2c]**. The fluorescence intensity is significantly decreased by LPS administration (11.74 ± 1.45, p<0.001) which is reverted back up to the control level by surfactant treatment (control = 22.69 ± 0.64; P-SF = 20.14 ± 0.20; S-SF = 18.11 ± 0.44, p<0.001, **Figure– 2d**).

3.3. Alterations in Ca^{2+} homeostasis

The fluorescence emission of CTC has been used to measure the level of divalent cations (specifically Ca^{2+} and Mg^{2+}) associated with envelope membranes in a wide range of animal cells. Images illustrating the cells taking up CTC dye (green fluorescence) in all the groups were shown in **Figure 3(a)**. Quantitative analysis showed 35.5% (p<0.001) of cells were CTC positive in LPS group as compared to 6.5% CTC positive cells in control group **[Figure– 3c]**. Both LPS+SF treated groups showed decreased percentage of CTC positive cells when comparisons were made with LPS group (20.25% in LPS+P-SF (p<0.001) and 21.25% (p<0.001) in LPS+P-SF).

The fluorescence signal was diminished significantly with LPS treatment (1.78 ± 0.39, p<0.001) in comparison to control group (4.40 ± 0.60) which indicates more Ca^{2+} displaced from the cell

IIOAB-India

Mittal et al. IIOABJ; Vol. 3; Issue 1; 2012:3–10 **5**

membrane to the cytosol with LPS whereas CTC bind to the membrane bound Ca^{2+} in control group (high fluorescence intensity, **[Figure– 3b]**. In surfactant treated groups, the LPS mediated fluorescence intensity was gradually increased with P-SF (3.05 ± 0.24, $p<0.001$) and S-SF (2.45 ± 0.11, $p<0.001$). Further, in this study the cytosolic Ca^{2+} concentration was measured in BALF cells with LPS treatment followed by exogenous surfactant (P-SF and S-SF). In contrast to control

group ($[Ca^{2+}]i = 50.12 \pm 1.51$ nM), LPS induced a gradual increase in $[Ca^{2+}]i$ (199.49 ± 0.96 nM, $p<0.001$) which is also consistent with the above result. In the presence of exogenous surfactants, the LPS-induced increase in $[Ca^{2+}]i$ was reduced by P-SF (143.95 ± 1.62 nM, $p<0.001$). Similarly, the LPS-induced $[Ca^{2+}]i$ was also markedly inhibited by the S-SF (172.28 ± 0.82 nM, $p<0.001$) as shown in **Figure– 3(d)**.
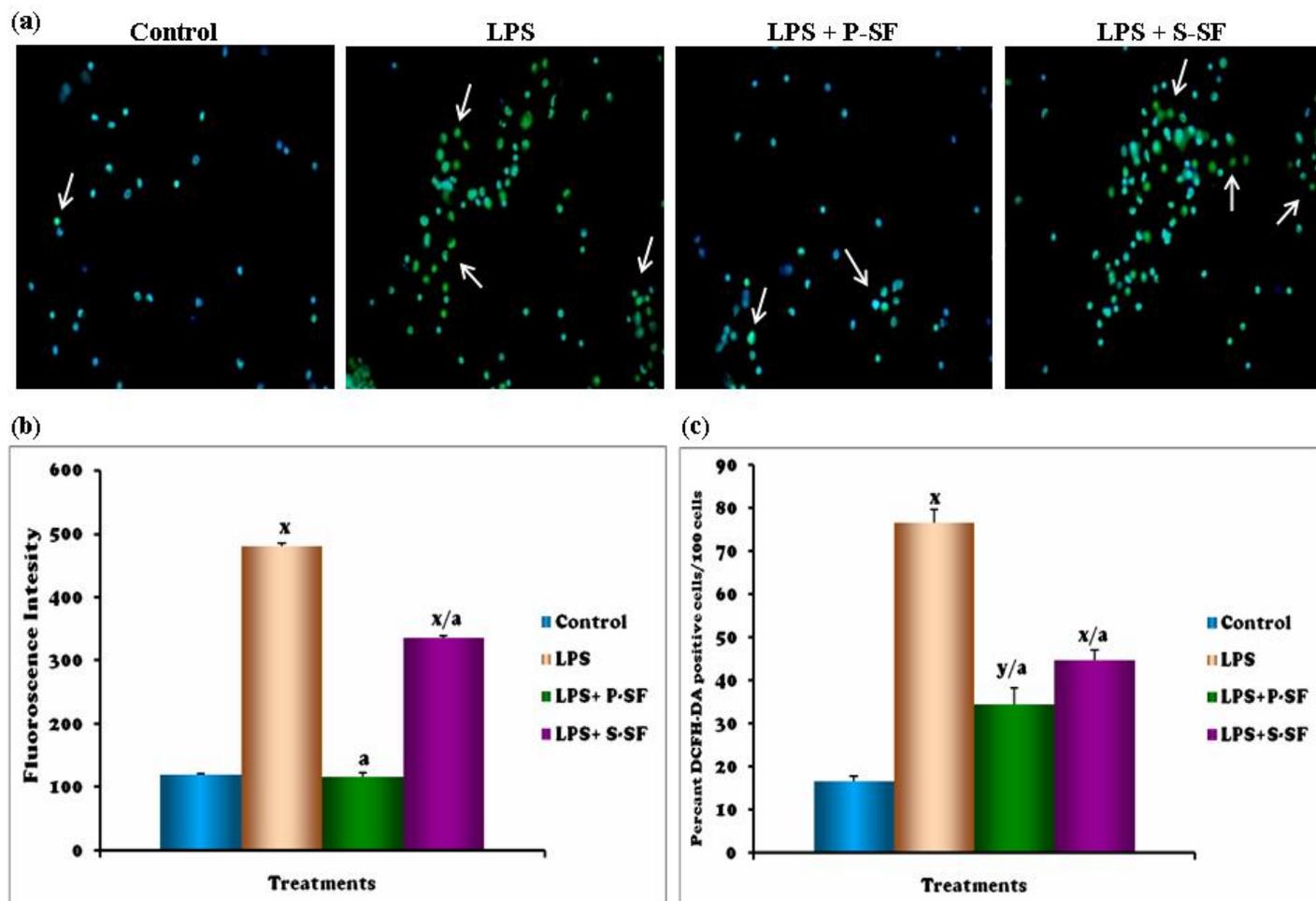

Fig. 1: (a) Images depict the morphological changes with the DCFH-DA dye in all the groups. **(b)** Quantitative analysis showed DCFH-DA positive cells. Values are mean ± S.D. of four independent observations, $^x p<0.001$ vs control; $^a p<0.001$ vs LPS.

### 3.4. Apoptosis by fluorescent dyes

Annexin V was used in conjunction to the vital dye propidium iodide (PI) to distinguish the apoptotic cells from necrotic or late stage apoptotic cells **[Figure– 4a]**. Based on binding of annexin V and PI, cells can be divided into three subpopulations, i.e. early apoptotic cells (annexin V positive, PI negative), late apoptotic cells (annexin V positive, PI positive) and necrotic cells (PI positive). In the LPS treatment group

54.25% of cells were positive for cell surface exposure of PS which mark them for early apoptosis **[Figure– 4b]** whereas only 13% apoptotic cells were found in control cells and many were PI positive. Mixed population of dual staining cells was seen with surfactant co-administration. The percentages of annexin V positive cells were reduced to 27.25% ($p<0.001$) in P-SF and to 33.5% ($p<0.001$) in S-SF group in comparison to LPS treatment.

IIOAB-India

Mittal et al. IIOABJ; Vol. 3; Issue 1; 2012:3–10   **6**

MOLECULAR CELL BIOLOGY

www.iioab.org

www.iioab.webs.com

THE IIOAB JOURNAL

[IV] DISCUSSION

Reactive oxygen species (ROS) have been implicated in a variety of pulmonary diseases including adult respiratory distress syndrome [20]. We examined ROS production in BALF cells using a fluorescent dye (DCFH-DA) and found that both the surfactants inhibited LPS stimulated ROS generation which is consistent with previous results as found in the rabbit alveolar macrophages [21]. This would suggest that surfactant has the inhibitory effects on the immediate inflammatory response. Similarly, in studies with natural surfactant with SP-B and SP-C versus synthetic surfactant both the surfactant types equally inhibited the human neutrophil respiratory burst [22]. In addition to causing direct injury to lung associated cells, ROS also involved in the regulation of signaling activity [23].

Mitochondria are primary sources of ROS inside the cells and in the course of signal transduction that leads to apoptosis, mitochondria may release pro-apoptotic molecules, which is accompanied by loss of the transmembrane potential ($\Delta\Psi$m) that can be detected by specific fluorescent probes [24]. Freshly isolated BALF cells showed a complex staining with JC-1, indicating an intricate network of mitochondrial structures exhibiting both red (high membrane potential) fluorescence and green (low mitochondrial membrane potential). The ratio of red to green fluorescence is a measure of the mitochondrial membrane potential. This pattern of regions of hyperpolarized and depolarized mitochondria has been reported in other cell types and is considered to reflect uneven distribution of proton circuits, respiration, ATP synthesis, and localized Ca^{2+} inside mitochondria [25].
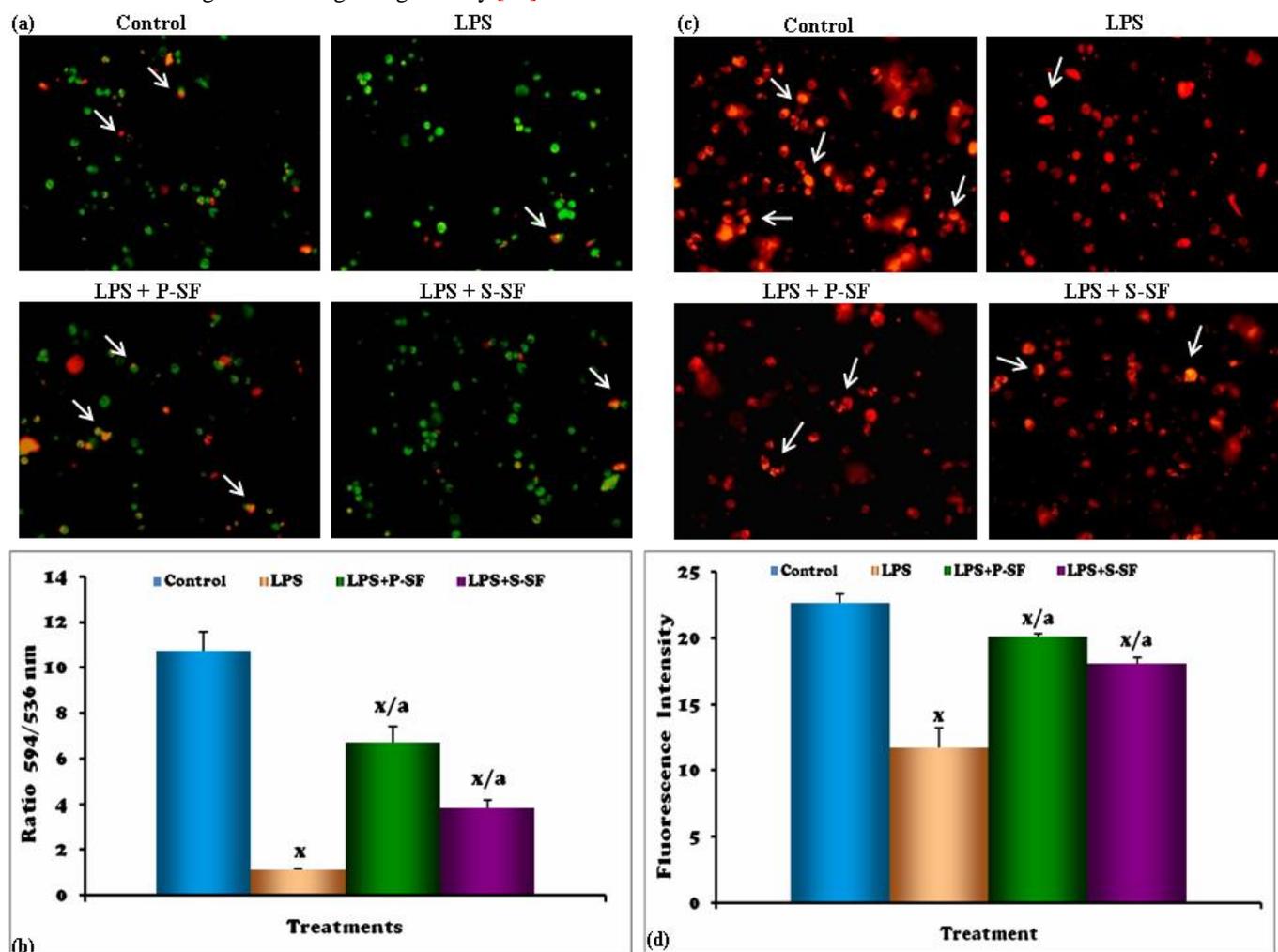
Fig. 2: **(a)** Changes in morphology of mitochondrial integrity in control, LPS-treated cells and with LPS + surfactant treatment precede **(b)** changes in mitochondrial membrane potential with JC-1. **(c)** Images with rhodamine-123 whereas **(d)** represents results from fluorometric analysis with rhodamine-123. Values are mean ± S.D. of four independent observations, [x]p<0.001, [y]p < 0.01 vs control; [a]p<0.001 vs LPS.

IIOAB-India

Mittal et al. IIOABJ; Vol. 3; Issue 1; 2012:3–10 **7**
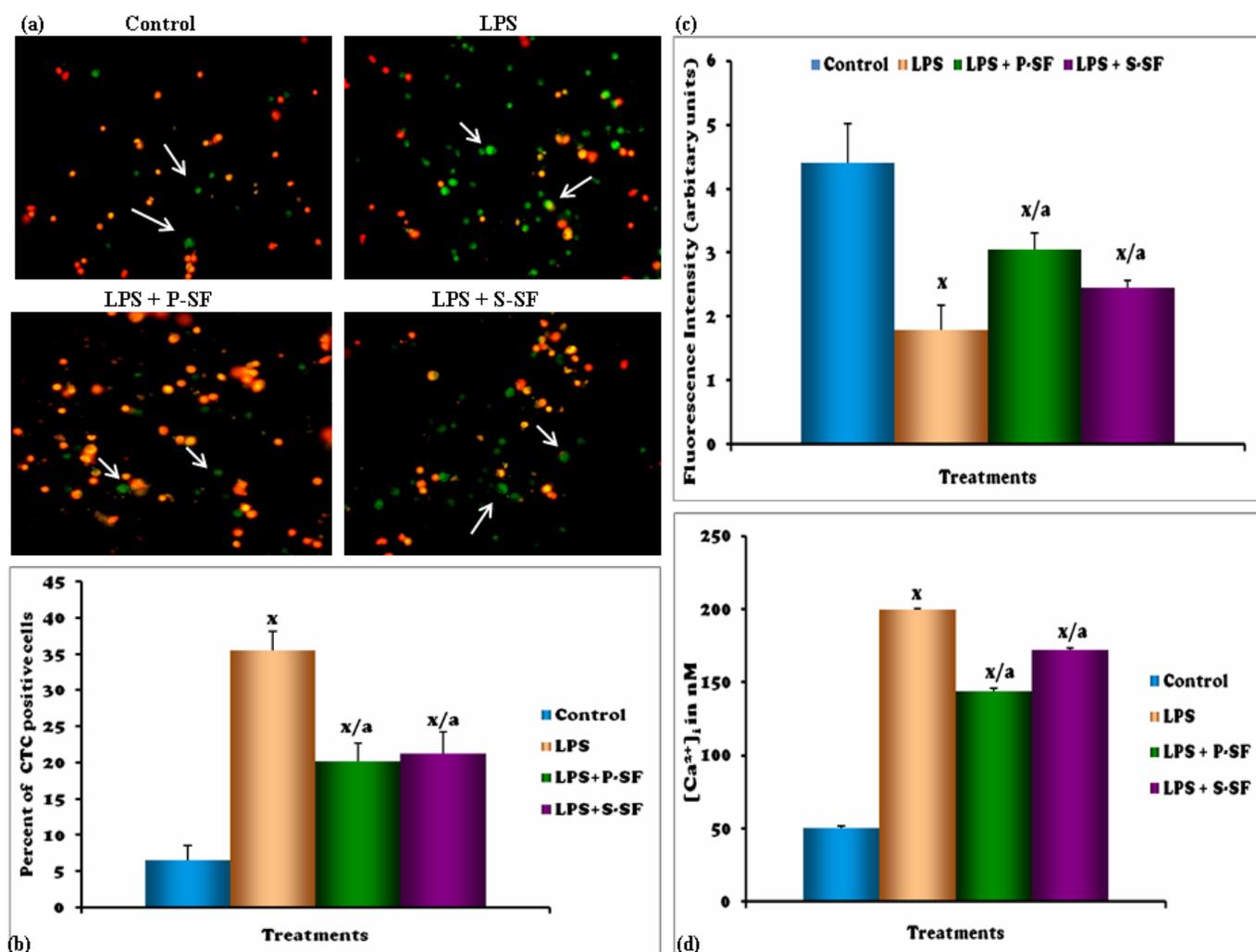
Fig. 3: (a) Images depict the effect of various treatments on CTC fluorescence. **(b)** Alterations in Ca^{2+} mobilization as measured with CTC fluorescence and **(c)** percentage of CTC positive cells/100 cells from four independent observations in each group **(d)** Intracellular calcium (nM) in BALF cells after LPS and surfactant treatments. Values are mean ± S.D. of four independent observations, [x]p<0.001 vs control; [a]p<0.001 vs LPS.

Mitochondrial dysfunction may also result through a change in cation homeostasis brought about by high ROS levels [26]. There are several lines of evidence to support strong role of Ca^{2+} [27]. CTC is a fluorescence-based stain, which forms chelate complexes in the presence of calcium ions in a 1:1 ratio [28]. When the CTC-calcium complex is mobilized from the highly lipophilic membrane environment to the more polar cytosol, there is a 100 fold decrease in the quantum efficiency of the indicator, which leads to a decrease in the observed fluorescence signal [29]. Calcium is released from the endoplasmic reticulum stores on stimulation of the cell, leading to a calcium influx across the plasma membrane via calcium channels [30]. Various pathogenic particles have been shown to produce changes in calcium flux within the cell [31] and a large

number of physiological and pathological cellular functions could be stimulated via calcium signaling. The release of pro-inflammatory mediators such as the cytokine TNF-α is driven by intracellular calcium related signaling pathways in diseases such as sepsis [32].

In the present study, the LPS treatment induces an elevation in $[Ca^{2+}]i$ in the BALF cells and such Ca^{2+} influx was inhibited by both animal derived and synthetic surfactants. Surfactant also inhibits Ca^{2+} influx in human neutrophils, possibly by membrane depolarization from insertion of surfactant-associated protein-dependent cation channels [33]. More recently, bovine-derived surfactants were found to directly increase neutrophil $[Ca^{2+}]i$ by releasing Ca_2+ from internal

IIOAB-India

Mittal et al. IIOABJ; Vol. 3; Issue 1; 2012:3–10 **8**

stores [34]. Therefore, blocking extracellular Ca^{2+} influx previously shown to modulate inflammatory response in peritoneal macrophages [35] may be an important mechanism regulating the anti-inflammatory properties of the exogenous surfactants. As measured in other trials, the phospholipids from both animal-derived and synthetic-surfactants demonstrate anti inflammatory properties. DPPC, the major phospholipid in natural and exogenous surfactants, similarly inhibited Ca^{2+} influx in the NR8383 AM cell line in an earlier study [36].
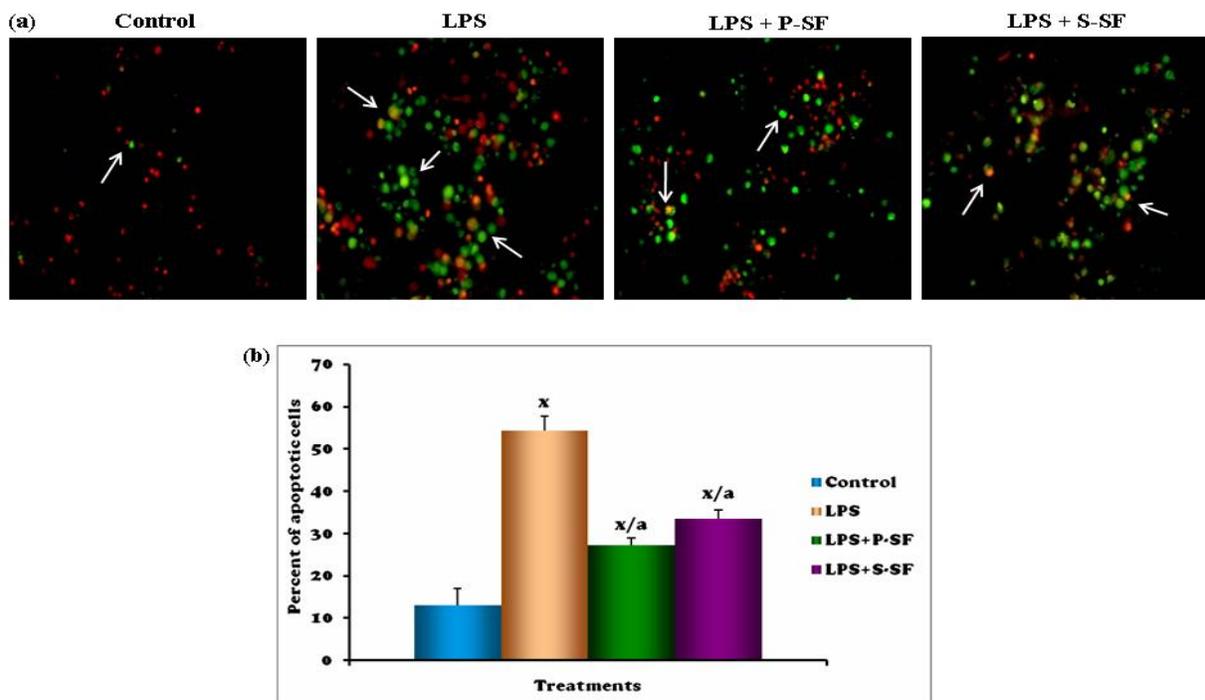
Fig. 4: (a) Photomicrograph showing apoptotic cells by staining with Annexin V and propidium iodide. **(b)** Quantitative analysis of the apoptotic cells, total 100 cells were counted in four different slides from each group and percent of apoptotic cells calculated. Values are mean ± S.D. of four independent observations, $^{x}p < 0.001$ vs control rats and $^{a}p < 0.001$ vs LPS rats.

[V] CONCLUSION

In conclusion, the explanation of the loss ΔΨm, associated with an increase in [Ca^{2+}]$_c$ is that H$_2$O$_2$ is placing stress on cellular energy store by driving down the ATP levels that would drive ATP synthesis and run down the electrochemical gradient. The Ca^{2+} influx coupled with release of Ca^{2+} from intracellular pools may provide a signal for the loss of ΔΨm that eventually leads to apoptosis-like death in LPS mediated ARDS model. Because mitochondrial changes brought about by ROS could be a crucial event in the pathogenesis of the disease, the effects of exogenous surfactant on elements in this signal transduction pathway may clarify its role of minimizing pulmonary inflammation associated with the ARDS.

ACKNOWLEDGEMENT

CONFLICTS OF INTERESTS

The authors report no conflicts of interest. The authors alone are responsible for the content and writing of the paper.

REFERENCES

[1]   Tang PS, Mura M, Seth R, Liu M. [2008] Acute lung injury and cell death: how many ways can cells die? *Am J Physiol Lung Cell Mol Physiol* 294:L632–L641.

[2]   Zamzami N, Marchetti P, Castedo M, Hirsch T, Susin SA, Masse B, Kroemer G. [1996] Inhibitors of permeability transition interfere with the disruption of the mitochondrial transmembrane potential during apoptosis. *FEBS Lett* 384:53–57.

[3]   Dvorakova K, Waltmire CN, Payne CM, Tome ME, Briehl MM, Dorr RT. [2001] Induction of mitochondrial changes in myeloma cells by imexon. *Blood* 11:3544–3551.

[4]   Thannickal VJ, Fanburg BL. [2000] Reactive oxygen species in cell signaling. *Am J Physiol Lung Cell Mol Physiol* 279:L1005–L1028.

MOLECULAR CELL BIOLOGY

IIOAB-India

Mittal et al. IIOABJ; Vol. 3; Issue 1; 2012:3–10

9

[5] Ide T, Tsutsui H, Hayashidani S, Kang D, Suematsu N, et al. [2001] Mitochondrial DNA damage and dysfunction associated with oxidative stress in failing hearts after myocardial infarction. *Circ Res* 88:529–535.

[6] Mayer B, Oberbauer R. [2003] Mitochondrial regulation of apoptosis. *News Physiol Sci* 18:89–94.

[7] Tagliarino C, Pink JJ, Dubyak GR, Nieminen AL, Boothman DA. [2001] Regulation of the p53 tumor suppressor protein. *J Biol Chem* 276:19150–19159.

[8] Kruman II, Mattson MP. [1999] Pivotal role of mitochondrial calcium uptake in neural cell apoptosis and necrosis. *J Neurochem* 72:529–540.

[9] Koya RC, Fujita H, Shimizu S, Ohtsu M, Takimoto M, Tsujimoto Y, Kuzumaki N. [2000] Gelsolin Inhibits Apoptosis by Blocking mitochondrial Membrane Potential Loss and Cytochrome c Release. *J Biol Chem* 275:15343–15349.

[10] Ward MW, Rego AC, Frenguelli BG, Nicholls DG. [2000] Mitochondrial membrane potential and glutamate excitotoxicity in cultured cerebellar granule cells. *J Neurosci* 20:7208–7219.

[11] Enhorning G. [1989] Surfactant replacement in adult respiratory distress syndrome. *Am Rev Respir Dis* 140:281–283.

[12] Spragg RG. [1995] Clinical results after natural and artificial exogenous surfactant therapy. *Appl Cardiopulm Pathophysiol* 5:116.

[13] Mittal N, Sanyal SN. [2010] Intratracheal Instillation of Surfactant Inhibits Lipopolysaccharide-induced Acute Respiratory Distress Syndrome in Rats. *Am J Biomed Sci* 2:190 – 201.

[14] Mittal N, Sanyal SN. [2009] Exogenous surfactant suppresses inflammation in experimental endotoxin-induced lung injury. l *J Enviorn Toxicol Pathol Onco* 28:341-349.

[15] Mittal N, Sanyal SN. [2010] Cyclooxygenase inhibition enhances the effects of surfactant therapy in endotoxin induced rat model of ARDS. *Inflammation* DOI: 10.1007/s10753-010-9211-6.

[16] Mittal N, Sanyal SN. [2010] Immunomodulatory properties of exogenous surfactant in adult rat alveolar macrophages. *Immunopharm Immunot* 32:153–159.

[17] Dey R, Moraes CT. [2000] Lack of Oxidative Phosphorylation and Low Mitochondrial Membrane Potential Decrease Susceptibility to Apoptosis and Do Not Modulate the Protective Effect of Bcl-xL in Osteosarcoma Cells. *J Biol Chem* 275:7087–7094.

[18] Dixon D, Brandt N, Haynes DH. [1984] Chlortetracycline fluorescence is a quantitative measure of the free internal $Ca2+$ concentration achieved by active transport. *J Biol Chem* 259:13737-13741.

[19] Grynkiewicz G, Poenie M, Tsien RY. [1985] A new generation of Ca_2+ indicators with greatly improved fluorescent properties. *J Biol Chem* 260:3440–3450.

[20] Hoidal JR. [2001] Reactive oxygen species and cell-signaling. *Am J Respir Cell Mol Biol* 25:661–663.

[21] Hayakawa H, Myrvik QN, St. Clair RW. [1989] Pulmonary surfactant inhibits priming of rabbit alveolar macrophage. Evidence that surfactant suppresses the alveolar macrophage in infant rabbits. *Am Rev Respir Dis* 140:1390–1397.

[22] Ahuja A, Oh N, Chao W, Spragg RG, Smith RM. [1996] Inhibition of the human neutrophil respiratory burst by native and synthetic surfactant. *Am J Resp Cell Mol Biol* 14:496–503.

[23] Sen CK, Packer L. [1996] Antioxidant and redox regulation of gene transcription. *FASEB J* 10:709–720.

[24] Cossarizza A, Kalashnikova G, Grassilli E, Chiappelli F, Salvioli S, Capri M, Barbieri D, Troiano L, Monti D, Franceschi C. [1994] Mitochondrial modifications during rat thymocyte apoptosis: a study at the single cell level. *Exp Cell Res* 214:323–330.

[25] Minamikawa T, Williams DA, Bowser DN, Nagley P. [1999] Mitochondrial permeability transition and swelling can occur reversibly without inducing cell death in intact human cells. *Exp Cell Res* 246:26–37.

[26] Duchen MR. [2000] Mitochondria and calcium: from cell signalling to cell death. *J Physiol* 529: 57–68.

[27] Hotchkiss RS, Osborne DF, Lappas GD, Karl IE. [1995] Calcium antagonists decrease plasma and tissue concentrations of tumor necrosis factor-α,interleukin-1β and interleukin-1α in a mouse model of endotoxin. *Shock* 3:337–432.

[28] Caswell AH, Hutchison JD. [1971] Selectivity of cation chelation to tetracyclines: evidence for special conformation of calcium chelate. *Biochem Biophys Res Commun* 43:625–630.

[29] Luthra R, Olson MS. [1978] The effects of chlorotetracycline on calcium movements in isolated rat liver mitochondria. Arch Biochem *Biophys* 191:494–502.

[30] Hoyal CR, Giron-Calle J, Forman HJ. [1998] The alveolar macrophage as a model of calcium signalling in oxidative stress. *J Toxicol Enviorn Health B Crit Care Rev* 1:117–134.

[31] Stone V, Brown DM, Watt N, Ritchie H, Wilson M, Donaldson K. [2000] Ultrafine particle-mediated activation of macrophages: intracellular calcium signalling and oxidative stress. *Inhale Toxicol* 12:345–351.

[32] Sayeed MM. [1996] Alterations in calcium signaling and cellular responses in septic injury. *New Horizons* 4:72–86.

[33] Chacon-Cruz E, Buescher ES, Oelberg DG. [2000] Surfactant Modulates Calcium Response of Neutrophils to Physiologic Stimulation via Cell Membrane Depolarization. *Pediatr Res* 47:405–413.

[34] Boston ME, Frech GC, Chacon-Cruz E, Buescher ES, Oelberg DG. [2004] Surfactant releases internal calcium stores in neutrophils by G protein-activated pathway. *Exp Bio Med* 229:99–107.

[35] Hotchkiss RS, Bowling WM, Karl IE, Osborne DF, Flye MW. [1997] Calcium antagonists inhibit oxidative burst and nitrite formation in lipopolysaccharide-stimulated rat peritoneal macrophages. *Shock* 8:170–178.

[36] Kerecman J, Mustafa SB, Vasquez MM, Dixon PS, Catro R. [2008] Immunosuppressive properties of surfactant in alveolar macrophage NR8383. *Inflamm Res* 57:118-125.

MOLECULAR CELL BIOLOGY

IIOAB-India

Mittal et al. IIOABJ; Vol. 3; Issue 1; 2012:3–10 **10**